ICEBERG SIZE AND ORIENTATION ESTIMATION USING SEAWINDS

Keith M. Stuart and David G. Long

Brigham Young University, MERS Laboratory, 459 CB, Provo, UT 84602

ABSTRACT

From 1999 to 2009, the SeaWinds scatterometer has been used to detect and track large Antarctic icebergs on a daily basis. Here, we develop an automated estimation algorithm to supplement iceberg position reports with estimates of the iceberg's major axis length, minor axis length, and angle of orientation. A maximum-likelihood objective function that relates measured backscatter to model-based simulated backscatter is developed. The utility of the estimation approach is analyzed in simulation and via a case study of iceberg A22a. Subsequent results agree with and supplement reports compiled by the United States National Ice Center.

Index Terms— Ice, radar scattering, estimation

1. INTRODUCTION

The SeaWinds scatterometer was originally designed to measure surface winds over the ocean. In addition to SeaWinds' primary goal, high-resolution data products enable valuable contributions to ice studies in the Antarctic. Even though SeaWinds was never designed to track icebergs, an extensive Antarctic iceberg database detailing positions of large tabular icebergs has been derived from the data and is used in this study. From high-resolution backscatter images, iceberg location and backscatter values can be extracted.

By utilizing backscatter differences in backscatter between glacial ice, sea ice, and sea water, it is possible to detect and track large Antarctic icebergs. These floating glacial ice fragments must generally be larger than 5 km to be detected and are typically characterized as a rough ice plateau above the water. Using reconstruction-enhanced scatterometer images, these icebergs are manually tracked on a daily basis and are cataloged as part of the Scatterometer Record Pathfinder Project at Brigham Young University's Microwave Earth Remote Sensing (MERS) Laboratory [1, 2, 3]. To supplement iceberg position reports, we would like to report iceberg size and angle of rotational orientation.

Here, we extend the analysis of SeaWinds iceberg observations to include size and orientation via maximum-likelihood (ML) estimation techniques. First, the background for large tabular iceberg observation by SeaWinds backscatter measurements is reviewed. Next, an elliptical model is chosen to characterize large tabular icebergs. An objective function relating measured backscatter given model-based backscatter is developed, based on the ML estimation approach. Next, the utility of the estimate is analyzed in simulation and a case study of iceberg A22a is presented. Finally, subsequent size and orientation estimates are compared with reports collected by the United States National Ice Center (NIC).

2. BACKGROUND

SeaWinds is a Ku-band scanning pencil-beam scatterometer aboard the QuikSCAT spacecraft and is designed to determine the normalized radar cross section, σ°, of the Earth's surface. Its sun-synchronous orbit allows for complete daily coverage of the polar regions, making it an ideal platform for high-latitude studies. SeaWinds has two scanning conical beams. The outer beam is vertically polarized at a nominal incidence angle of 54°; the inner beam is horizontally polarized at a nominal incidence of 46°. This design provides for four independent looks of the region lying within the inner swath and two independent looks of targets contained within the outer swath [4, 5].

Using onboard range-Doppler processors, SeaWinds backscatter values for each microwave pulse are separated into regions called slices where each has a separate σ° value. Because of the rapid roll-off of the aperture response function corresponding to each slice, individual

response patterns are frequently represented as a binary mask corresponding to the 6 dB contour of each slice footprint, measuring approximately 6 x 25 km.

Because each range-Doppler-filtered slice has a large spatial footprint compared to the operating wavelength, each σ° measurement may be modeled as a linear combination of spatial backscatter distributions where

$$\sigma^\circ = \frac{\int A(\tau)\sigma^\circ_{pt}(\tau)d\tau}{\int A(\tau)d\tau} + \nu \tag{1}$$

where σ° is a SeaWinds backscatter measurement, $A(\tau)$ is the antenna gain of the 2-dimensional ground illumination footprint, $\sigma^\circ_{pt}(\tau)$ is the spatial distribution of σ° at the surface, and ν is the effective noise term.

3. THEORY

Rather than use backscatter images as done previously, the proposed approach uses individual slice measurements and their binary spatial response functions. Backscatter values are collected around an iceberg such that the iceberg and the immediately-surrounding background sea water or sea ice is observable. In the local area, the backscatter values from the iceberg and the background are assumed to be spatially homogeneous. Given this assumption, Eq. 1 simplifies to

$$\sigma^\circ = c\sigma^\circ_{berg} + (1-c)\sigma^\circ_{back} + \nu. \tag{2}$$

where σ°_{berg} and σ°_{back} represent the average backscatter values of the iceberg and the surrounding medium (sea water or sea ice), c is the ratio of the ground spatial footprint over glacial ice to the background area and ν is the cumulative noise term.

Due to noise, the probability distribution of each σ° measurement is normally distributed according to

$$f(\sigma^\circ|\sigma^\circ_t) = \frac{1}{\sqrt{2\pi}\eta} exp\left\{-\frac{(\sigma^\circ - \sigma^\circ_t)^2}{2\eta^2}\right\} \tag{3}$$

where σ°_t is the true backscatter value and η is the variance of σ° [5].

A simple model is chosen to describe the area and approximate shape of a large tabular iceberg. This model is a super-ellipse of form

$$\left|\frac{x-x_c}{a}\right|^n + \left|\frac{y-y_c}{b}\right|^n = 1 \tag{4}$$

where x_c and y_c are the center parameters, a and b are the major and minor axis lengths and n is the super-ellipse parameters where $n > 0$. While irregularly shaped icebergs are not elliptical, this model is effective in generalizing iceberg shape for purposes of parameter estimation. The model parameters consist of those defined in Eq. 2 and 4, specifically σ°_{berg}, σ°_{back}, c, x_c, y_c, a, b, n, and an angle parameter for the iceberg rotational orientation. These parameters constitute the vector $\bar{p}$, the model parameter vector to estimate.

The estimation process is characterized by minimizing the difference between the measured backscatter and the model-based backscatter by adjusting model parameters. For a single radar measurement, this probability distribution is

$$f(\sigma^\circ|\sigma^\circ_s(\bar{p})) = \frac{1}{\sqrt{2\pi}\eta_s} exp\left\{-\frac{[\sigma^\circ - \sigma^\circ_s(\bar{p})]^2}{2\eta_s^2}\right\} \tag{5}$$

where σ° is the backscatter value measured by SeaWinds and σ°_s is the model-based backscatter based upon $\bar{p}$ from Eq. 4.

For multiple independent radar measurements, the joint distribution of σ° given $\sigma^\circ_s(\bar{p})$ is a joint distribution of independent random variables of form

$$f(\bar{\sigma}^\circ|\bar{\sigma}^\circ_s(\bar{p})) = \prod_j f(\sigma^\circ_j|\sigma^\circ_{s,j}(\bar{p})) \tag{6}$$

where j is the count of σ° measurements in the frame of estimation and $\bar{\sigma}^\circ$ and $\bar{\sigma}^\circ_s(\bar{p})$ represent vectorized forms of σ° and $\sigma^\circ_s(\bar{p})$, respectively.

Maximizing Eq. 6 yields a ML objective function. However for practical purposes, we maximize the log of Eq. 6. Furthermore, we are interested in the parameter vector $\bar{p}$ that maximizes Eq. 6. Therefore, the ML estimate of $\bar{p}$ may be expressed as

$$\bar{p}^* = \underset{\bar{p}}{argmax} \sum_j \left[-\frac{[\sigma^\circ - \sigma^\circ_s(\bar{p})]^2}{2\eta_s^2} - \ln(\sqrt{2\pi}\eta_s)\right] \tag{7}$$

where optimal model parameters are denoted $\bar{p}^*$.

For the noise-free case, Eq. 7 has a single maxima which is found by searching $\bar{p}$. However in a noisy environment, Eq. 7 is not guaranteed to have a single solution; therefore, an exhaustive search of $\bar{p}$ is conducted.

Figure 1a illustrates a simulated iceberg in a noise-free environment. The 6 dB-contour of the forward and aft-looking slice aperture responses over the iceberg

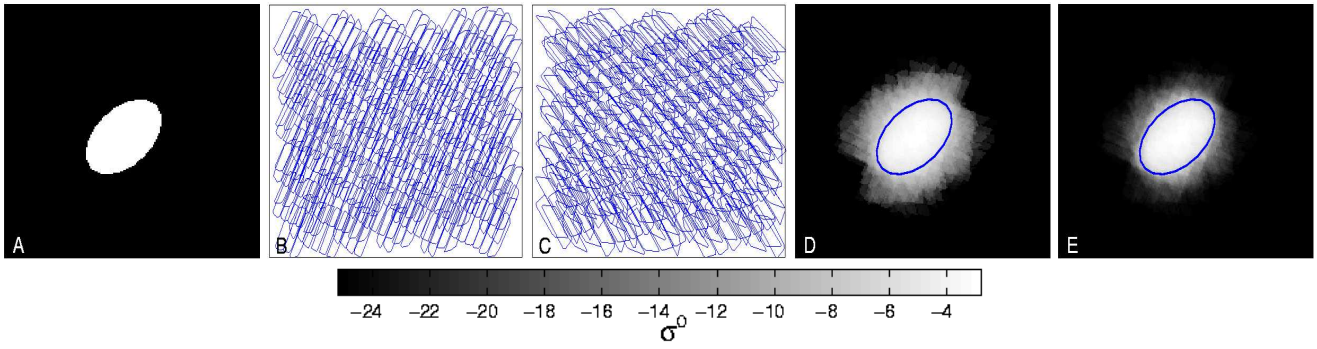

Fig. 1. Simulation of estimating the size and orientation of an elliptical iceberg. A) The initial binary iceberg model. B) 6 dB-contour plot of the forward-looking SeaWinds slice measurements for a single pass. There are approximately 330 slices, each approximately 25 x 6 km in dimension. C) Corresponding aft-looking slice measurements for the same pass. D) Geometric-average backscatter composite in dB. E) Geometric-average composite in linear space. Estimated parameters conformed exactly to the initial model parameters and corresponding elliptical shapes are juxtaposed over each composite image. Images correspond to approximately 300 x 300 km.

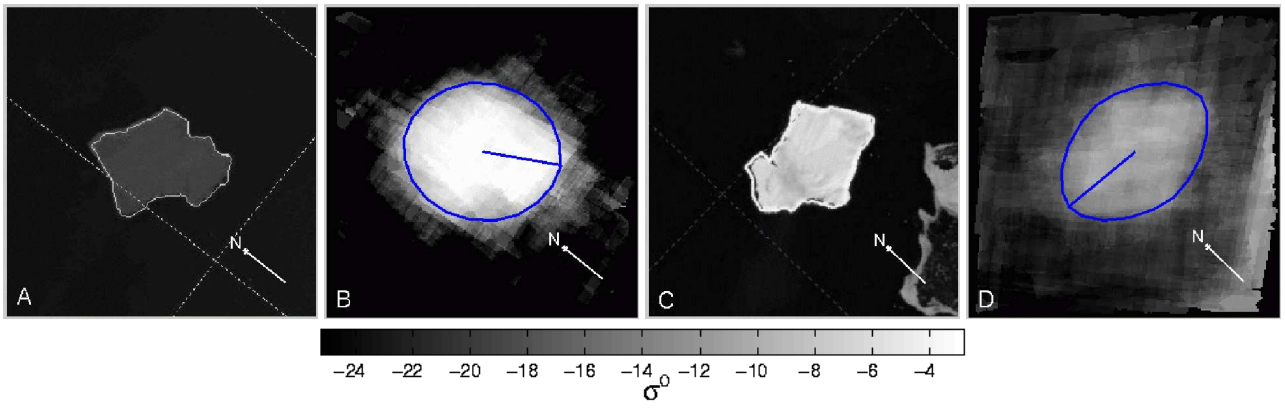

Fig. 2. Images of iceberg A22a on a) 2006JD110 from DMSP IR and c) 2006JD303 from MODIS. Corresponding horizontally-polarized SeaWinds backscatter images are in (b,d). Elliptical shapes based on the ML estimates of iceberg size and orientation are juxtaposed on the backscatter images. On JD303, iceberg σ° is lower due to surface melt conditions. Also, ocean σ° is higher due to increased surface roughness caused by local high wind conditions. For iceberg size comparisons, see Table 1.

Table 1. Major and minor axis comparisons of iceberg A22a between NIC reports and SeaWinds estimates on 2006 Julian Days 110 and 303.

	2006JD110		2006JD303	
	Major Axis	Minor Axis	Major Axis	Minor Axis
NIC Report	68 km	51 km	68 km	51 km
SeaWinds ML Estimate	66 km	57 km	70 km	49 km
Percent Error	3%	12%	3%	4%

for a single pass are displayed in Fig. 1b,c. Composite backscatter images are displayed in Fig. 1d,e for the linear and geometric average cases in both dB and linear space. The elliptical shapes correspond to the ML estimates of the major axis, minor axis, and angle of rotation. As expected, estimated parameters converge to the initial model parameters. Notice that the geometric average backscatter image displayed in linear space more closely resembles the true iceberg profile in Fig. 1a.

4. CASE STUDY

The technique is applied to SeaWinds backscatter measurements of iceberg A22a. Iceberg A22a is selected because it is non-circular, is tracked for an extended period of time away from sea ice, and because collocated high-resolution imagery is available.

Two days are highlighted in this study: 2006 JD 110 and 303. For these days, annotated high-resolution images of iceberg A22a are available from DMSP and MODIS and are displayed in Fig. 2a,c. Corresponding SeaWinds backscatter measurements for these days and are displayed in Fig. 2b,d. Elliptical shapes based on iceberg size and orientation estimates are also juxtaposed on the backscatter images. NIC reports and SeaWinds estimates are compared in Table 1. Note the consistency of iceberg orientation in the high-resolution images and the ML estimates. ML estimates coincide with iceberg dimensions reported by the NIC via high-resolution imagery to within an average of 94%.

5. CONCLUSION

A maximum-likelihood objective function that relates measured backscatter to an iceberg model is developed. This technique is used to successfully estimate iceberg size and rotational orientation in both a simulated environment and via a case study of iceberg A22a. The estimates coincide to dimensions reported by the NIC via high-resolution imagery with 94% accuracy. This technique provides iceberg size and orientation which was only previously available from high-resolution sensors. As a result, the daily evolution of iceberg dimensions and rotational orientation over time may be explored using scatterometer data.

6. REFERENCES

[1] D. Long, J. Ballantyne, and C. Bertoia, "Is the Number of icebergs Really increasing?," *EOS Transactions of the American Geophysical Union*, vol. 83, no. 42, pp. 469 474, Oct 2002.

[2] Microwave Earth Remote Sensing Laboratory, "Scatterometer Climate Record Pathfinder," http://www.scp.byu.edu/, update 2010.

[3] K.M. Stuart and D.G. Long, "Tracking large tabular icebergs using the SeaWinds Ku-band microwave scatterometer," *Deep Sea Research Part II: Topical Studies in Oceanography*, to appear, 2010.

[4] D.S. Early and D.G. Long, "Image Reconstruction and Enhanced Resolution Imaging from Irregular Samples," *IEEE Transactions on Geoscience and Remote Sensing*, vol. 39, no. 2, pp. 291–302, 2001.

[5] M.W. Spencer and D.G. Long, "Improved Resolution Backscatter Measurements with the SeaWinds Pencil-Beam Scatterometer," *IEEE Transactions on Geoscience and Remote Sensing*, vol. 38, no. 1, pp. 89–104, 2000.